Environmental Management (2014) 54:98–111
DOI 10.1007/s00267-014-0279-x

Integrating Satellite Imagery with Simulation Modeling to Improve Burn Severity Mapping

Eva C. Karau · Pamela G. Sikkink · Robert E. Keane · Gregory K. Dillon

Received: 24 May 2013 / Accepted: 11 April 2014 / Published online: 11 May 2014

Abstract Both satellite imagery and spatial fire effects models are valuable tools for generating burn severity maps that are useful to fire scientists and resource managers. The purpose of this study was to test a new mapping approach that integrates imagery and modeling to create more accurate burn severity maps. We developed and assessed a statistical model that combines the Relative differenced Normalized Burn Ratio, a satellite image-based change detection procedure commonly used to map burn severity, with output from the Fire Hazard and Risk Model, a simulation model that estimates fire effects at a landscape scale. Using 285 Composite Burn Index (CBI) plots in Washington and Montana as ground reference, we found that an integrated model explained more variability in CBI ($R^2 = 0.47$) and had lower mean squared error (MSE $= 0.28$) than image ($R^2 = 0.42$ and MSE $= 0.30$) or simulation-based models ($R^2 = 0.07$ and MSE $= 0.49$) alone. Overall map accuracy was also highest for maps created with the Integrated Model (63 %). We suspect that Simulation Model performance would greatly improve with higher quality and more accurate spatial input data. Results of this study indicate the potential benefit of combining satellite image-based methods with a fire effects simulation model to create improved burn severity maps.

Keywords Burn severity mapping · Fire effects · Modeling · RdNBR

E. C. Karau (✉) · P. G. Sikkink · R. E. Keane · G. K. Dillon
USDA Forest Service, Rocky Mountain Research Station, Missoula Fire Sciences Laboratory, 5775 Hwy 10 W, Missoula, MT 59808, USA
e-mail: ekarau@fs.fed.us

Introduction

Recognizing the importance of burn severity maps for a variety of fire management applications, scientists and land managers strive to develop more accurate and effective mapping methodologies. Currently, the most widely used approach to creating burn severity maps is with satellite imagery-based change detection methods. Studies conducted in a variety of landscapes have evaluated image-based approaches to burn severity mapping in the US and internationally (see French et al. 2008 for more detail). Other studies have employed the approach to investigate research questions requiring a spatial assessment of burn severity (Miller et al. 2009b; Epting and Verbyla 2004; Collins et al. 2007; Haire and McGarigal 2009; Dillon et al. 2011a). Additionally, the Monitoring Trends in Burn Severity project is a multi-agency effort initiated to produce a national scale fire atlas based on satellite derived burn severity maps (Eidenshink et al. 2007).

A field-based assessment of burn severity that is designed to aid in calibration and validation of satellite-based severity maps is the composite burn index (CBI) (Key and Benson, 2006a). Many studies have found correlations between CBI and burn severity measurements derived from satellite imagery (see French et al. 2008). Other studies have revealed relationships between image-based metrics and specific measurable fire effects to surface, understory, and overstory vegetation (Karau and Keane 2010; Hudak et al. 2007; Miller et al. 2009a; Keeley et al. 2008).

However, despite correlations between satellite-based severity metrics and field-measured fire effects, image-based tools use passive sensors that detect light reflectance; they do not directly measure any biophysical process or fire effect on vegetation (Jensen 1983). Simulation modeling, on the other hand, produces estimates of biophysical fire effects. One example of a simulation model that can produce maps of predicted first order fire effects is the Fire Hazard and Risk Model (FIREHARM). FIREHARM is a cross-platform C++ program that functions as a landscape-scale spatial fire effects research model and generates maps of physically based estimates of fire effects such as damage to trees, understory vegetation, litter, duff, and soil at the spatial resolution of the input data (Keane et al. 2010). FIREHARM requires several input data layers to compute spatial fire effects variables. The most important model inputs for this study include digital maps of topography, vegetation, and fuels, along with site-specific weather and fuel moisture estimates. These inputs are passed to the First Order Fire Effects Model (FOFEM; Reinhardt et al. 1997) which includes a collection of quantitative predictive equations gleaned from the body of fire effects literature. FOFEM algorithms are embedded in the FIREHARM program to simulate estimates of tree mortality, fuel consumption, smoke emissions, and soil heating. Modeling these direct fire effects enables mapping of simulated wildfire effects and burn severity assessments that can be tailored for specific management applications.

As FIREHARM simulates the effect of fire on ecosystem components, it should not be confused with radiative transfer modeling, an approach that simulates optical properties of leaves or canopies that are used to classify satellite imagery into burn severity maps (Chuvieco et al. 2006; De Santis et al. 2009, 2010). Though both methods are referred to as “simulation modeling,” they are very different; FIREHARM simulates ecosystem response, while radiative transfer modeling simulates reflectance, and thus ultimately relies upon information captured by a remote sensing instrument. In this paper, the terms “simulation” and “modeling” refer to simulation of the direct effect of fire on vegetation.

In a preliminary comparison of the two methods, Karau and Keane (2010) found that both image-based and simulation-based burn severity mapping approaches have strengths and limitations associated with data availability, user expertise, production time, and accuracy. Satellite image-based methods provide a “view” of the change in a landscape due to fire, while fire effects simulation modeling could provide land managers with biophysically based estimates of fire effects across a landscape.

The purpose of this paper is to determine the potential of simulation modeling to add value to spatial burn severity assessments. We compared burn severity values estimated from (1) simulation modeling techniques, (2) satellite imagery-based mapping, and (3) an integration of both technologies, focusing on fires in conifer forests of the northwestern United States. Using the CBI field assessment of burn severity (Key and Benson, 2006a) as field validation, our objective was to merge the simulation and image-based approaches to create a statistical model that generates biophysically centered depictions of landscape burn severity.

Methods

Study Areas

We selected 15 wildfires that burned in coniferous forests of western Montana and central Washington between 2003 and 2009 to use in our comparison (Fig. 1). We chose fires where both georeferenced CBI data and satellite-based severity maps were available. These fires occurred in a variety of coniferous forests from low elevation, dry ponderosa pine to upper elevation Englemann spruce-subalpine fir (*Picea engelmannii-Abies lasiocarpa*), and lodgepole pine (*Pinus contorta*), with the majority of plots located in Interior Douglas-fir (*Pseudotsuga menziesii*) (Fig. 2). All sites can be described by a cool temperate climate with minor maritime influence and have mean annual temperatures ranging from 2 to 8 °C. All of our sites experience similar seasonal timing of precipitation, with relatively dry summers and most moisture coming as snow in the fall to spring months. Annual precipitation amounts, however, vary widely from 410 mm to over 2250 mm annually (McNab and Avers 1994; Western Regional Climate Center 2012). While all fires selected for this study burned during a similar time of year, differences in elevation, vegetation, total fire size, and burning conditions (Tables 1, 2) resulted in a wide range of fire effects and burn severities to facilitate our comparison of field data, simulation model output, and satellite imagery.

Field Reference Data

Our comparison of image-based and model-based burn severity mapping methods required a field-based measure of burn severity to serve as ground validation. Composite Burn Index (CBI) is a ground-based, synoptic burn severity measure that was developed to calibrate and validate image-based burn severity mapping tools (Key and Benson 2006a). CBI is used in this study to compare the three technologies: imagery, modeling, and their integration. CBI consists of several visual estimates and descriptions of fire damage on each of five distinct strata within the burned area of the forest. These strata are layered vertically from the forest floor upward and are: (a) the substrate, which includes soil and rock cover, duff, and surface fuels; (b) herbs, low shrubs, and trees less than 1 m; (c) tall shrubs and trees up to 5 m; (d) subcanopy trees; and (e) upper canopy trees. Each stratum incorporates four or

Fig. 1 Study areas showing locations of wildfires (*stars*) and weather stations (*diamonds*). CBI plot locations are not shown at this scale

five variables and ranks those variables on a continuous scale between zero and three. Values for all recorded variables across all strata are averaged to create a severity index value for the whole plot ranging between zero (unburned) and three (highest severity). Although CBI includes fire effects to soils, the index is heavily weighted to measuring fire effects to vegetation (Miller and Thode 2007).

CBI data for all 15 wildfires were evaluated using standard methods described by Key and Benson (2006a) in an Extended Assessment, where CBI was evaluated approximately 1 year post-fire. We obtained CBI data for Montana wildfires from studies on burn severity at the USDA Forest Service's Missoula Fire Sciences Laboratory (Keane et al. 2010; Karau and Keane 2010; Dillon et al. 2011b). For the Washington wildfires, CBI data came from field work conducted by researchers at the University of Washington and the USDA Forest Service's Pacific Wildland Fire Sciences Laboratory (Cansler 2011; Kopper 2012; Prichard et al. 2010). We used the overall CBI rating

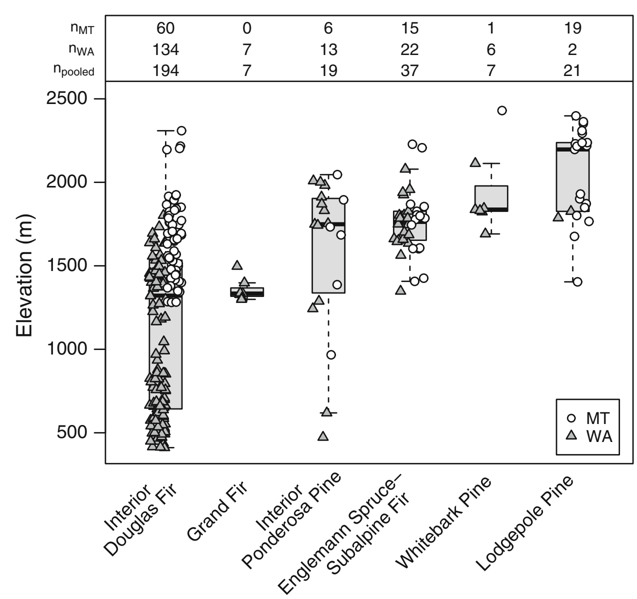

Fig. 2 Plot distribution throughout vegetation types

(continuous zero to three scale) from each plot, as the response variable in our statistical modeling. We also assigned each plot to a four category ordinal burn severity class using standard break points in the CBI scale (Key and Benson 2006a; Miller and Thode 2007).

Satellite Imagery

A common image-based methodology uses the Normalized Burn Ratio (NBR), a linear combination of Landsat wavelength bands four and seven calculated on single-date imagery, to map fire severity. When NBR images are produced before and after a fire, the images can be differenced to enhance the contrast between pre- and post-fire conditions, resulting in the Differenced Normalized Burn Ratio (dNBR) (Key and Benson 2006b). The dNBR has been successfully correlated with the CBI, a field-based integrative assessment of burn severity (Key and Benson 2006a).

Recent studies show that an adjustment to the dNBR calculation removes bias from the amount of pre-fire vegetation cover to provide a relative, rather than an absolute measure of the changes in vegetation between pre- and post-fire imagery (Miller and Thode 2007). This adjustment is the relative differenced NBR (RdNBR), which is calculated as follows:

$$RdNBR = \frac{\mathrm{dNBR}}{\sqrt{\mathrm{ABS}\left(\frac{\mathrm{prefireNBR}}{1000}\right)}} \qquad (1)$$

where ABS is the absolute value; dNBR is the pre-fire NBR value minus the post-fire NBR value; and pre-fire NBR value calculated by (Band4 − Band7)/(Band4 + Band7) of the Landsat TM image. For this study, we chose to use RdNBR as opposed to dNBR, because RdNBR is a relative measure of burn severity, and because it is more regionally consistent in its relationship to field-measured burn severity (Zhu et al. 2006; Miller and Thode 2007).

We obtained RdNBR for all 15 wildfires from the Monitoring Trends in Burn Severity (MTBS) website (http://www.mtbs.gov/). The MTBS project provides consistent, 30-meter resolution burn severity data and fire perimeters for all large fires in the United States (>405 ha in the western U.S., >202 ha in the eastern U.S.; Eidenshink et al. 2007). Using standard USGS image processing methodology (http://www.mrlc.gov/pdf/image_processing.pdf), MTBS acquires and processes pre-fire and post-fire Landsat TM and ETM+ imagery, from which they produce two continuous burn severity indices. We used the continuous RdNBR as the predictor variable in the imagery-based statistical model.

FIREHARM Input Data

We obtained FIREHARM digital map inputs of topography (elevation, slope, and aspect), vegetation (cover type and tree attributes), and fuels (fuel loading models) from the National LANDFIRE Mapping Project (www.landfire.gov). LANDFIRE is a joint project between the USDA Forest Service and US Department of Interior that produces a consistent set of 30-meter resolution geospatial data layers representing topography, vegetation, and fuels across the United States

Table 1 Characteristics of the wildfires from Montana and Washington

Fire_name	State	Area burned km^2 (acres)	Fire year	Start date[a]	Wind speeds[a] km hr^{-1} (m hr^{-1})	100 % contained[a]	Nearest weather station	Total CBI field plots
Bielenburg	MT	5.99 (1,480)	2009	12-Jul-09	3–64 (2–40)	23-Oct-09	Pburg (20 km)	6
Cooney Ridge	MT	104.17 (25,740)	2003	8-Aug-03	8–24 Gust48 (5–15 Gust30)	31-Dec-03	Lincoln (74 km)	26
Gash Creek	MT	39.98 (9,880)	2006	24-Jul-06	2–24 G48 (1–15 G30)	8-Dec-06	Smith Creek (0.8 km)	5
Gird End	MT	13.23 (3,270)	2009	9-Sep-09	14.5–24 (9–15)	26-Oct-09	Gird (6 km)	9
Jocko Lakes	MT	143.91 (35,560)	2007	31-Aug-07	64 (40)	4-Dec-07	Pistol Creek (21 km)	13
Kootenai Creek	MT	34.03 (8,410)	2009	12-Jul-09	3–24 (2–15)	31-Nov-09	Ninemile (55 km)	14
Lily Lake	MT	8.17 (2,020)	2009	13-Aug-09	8–48 (5–30)	16-Oct-09	French Creek (40 km)	9
Mineral Primm	MT	84.53 (20,890)	2003	6-Aug-03	5–48 G16 (3–30 G10)	31-Dec-03	Lincoln (77 km)	25
MP Boles Meadow	MT	17.36 (4,290)	2003	8-Aug-03	8–16 G40 (5–10 G25)	23-Aug-03	Lincoln (77 km)	3
Tarkio I90 Complex	MT	44.31 (10,950)	2005	4-Aug-05	5–32 G26 (3–20 G16)	17-Aug-05	Ninemile (13 km)	9
Camel Humps	WA	0.53 (130)	2008	23-Jul-08	not available	1-Aug-06	Stehekin Airstrip (11 km)	28
Cold Springs	WA	31.28 (7,729)	2008	12-Jul-08	5–45 G29 (3–28 G18)	1-Aug-08	Sawmill (96 km)	28
Flick Creek	WA	28.53 (7,050)	2006	26-Jul-06	2–24 G40 (1–15 G25)	19-Oct-06	Stehekin Airstrip (5 km)	100
Tripod	WA	241.64 (59,710)	2006	24-Jul-06	0–16 G21 (0–10 G13)	9-Nov-06	First Butte (0.8 km)	14
Tripod Spur Peak	WA	465.88 (115,120)	2006	3-Jul-06	3–16 G16 (2–10 G10)	9-Nov-06	First Butte (0.8 km)	29

[a] Based on the National Incident Management Coordination Center (*NIMCC*) incident management situation reports

(Rollins 2009). We obtained fuel loading input data from the LANDFIRE FLM (Fuel Loading Model) product (Reeves et al. 2006). FLMs are categories in a national classification of fuelbeds that were built to meet the resolution of the FOFEM model, and each FLM category has a unique set of loadings for all fuel components needed to compute fuel consumption and smoke emissions (Lutes et al. 2009; Sikkink et al. 2009). We computed fire behavior using the LANDFIRE data layer derived from fire behavior fuel models (Anderson 1982). To compute tree mortality, we used tree data from the National Tree List database (Drury and Herynk 2011), also linked to LANDFIRE. We used two versions of the LANDFIRE data; for fires that occurred prior to 2008, we used LANDFIRE 2001 "Refresh" (LF_1.0.5) and for fires that occurred after 2008, we used LANDFIRE 2008 "Refresh" (LF_1.1.0).

The remaining FIREHARM inputs were site-specific weather variables that control fuel moistures and burn conditions (Table 2). We obtained local weather conditions during the fire from the weather stations nearest to the fire; distance from fire to weather station ranged from 0.8 to 96 km (Table 1). We calculated fuel moistures for the 1-, 10-, 100-, 1,000-hr, herb, and shrub components within Fire Family Plus (Bradshaw and Tirmenstein 2010) using daily weather observations for the fire dates. We calculated moisture values for the fine fuels (1 and 10 h) within Fire Family Plus using hourly moisture data from the Western Regional Climate Center (Western Regional Climate Center 2012) starting 2 weeks prior to the date of the fire and continuing until containment (minimum of 90 %). For this we used the Nelson fuel moisture model (Nelson 2000; Carlson et al. 2007), which is the most recently accepted method to compute fine fuel moistures. We calculated duff moistures using the Canadian Forest Fire Weather Index System (Van Wagner and Pickett 1985) from daily data using the date, dry bulb temperature, relative humidity, and precipitation amount and started on May 1 of each year to allow for calibration. We set live foliar moisture at 100 % in Fire Family Plus, and we set litter moisture equal to the 1-hr fuel moistures. We averaged all weather and fuel values for the duration of the fire to create a single value for each parameter to populate FIREHARM's weather and fuel moisture input file.

Statistical Modeling

We built several statistical models using CBI as the response variable. We used linear and nonlinear regression to explore the relationship between CBI and RdNBR, and we used multiple linear regression analysis to characterize the relationships between CBI and simulated fire effects variables, and CBI and an integration of RdNBR and simulated variables. Exploratory data analysis showed minimal differences in both the distribution of plots throughout forest types (Fig. 2) and in the CBI-RdNBR linear regression relationship for Montana versus Washington (Fig. 3), so we did not geographically stratify the analysis. We used R (R Development Core Team 2010) software for all statistical analyses.

RdNBR Linear and Nonlinear Models

Some studies that have assessed the relationship between CBI and satellite-based burn severity indices have used CBI as the response variable (van Wagtendonk et al. 2004; Cocke et al. 2005; Holden et al. 2009; Soverel et al. 2010), while others have used CBI as the predictor variable (in that case, with the satellite index as the response) (Miller and Thode 2007; Miller et al. 2009a, b; Dillon et al. 2011a; Cansler and McKenzie 2012). Although Cansler and McKenzie (2012) make a strong case for why CBI should be used as the predictor, we used it as the response to facilitate the comparison of technologies, because it is the one common variable across the three approaches. This is supported by the fact that in other studies that have evaluated the use of modeling and satellite imagery to measure burn severity, CBI has been used as the response in regression models (Chuvieco et al. 2006; De Santis et al. 2009, 2010). We evaluated both linear and nonlinear models to represent the relationship between CBI-RdNBR; we present results of the linear relationship between CBI and RdNBR for thoroughness and consistency with simulated and integrated models, which are also linear. Assessment of model residuals indicated that residuals were normally distributed for both linear and nonlinear CBI-RdNBR models.

Simulated Variables Models

We selected the following FIREHARM outputs to build a statistical model for simulated burn severity, because we thought they best represented the gradients of burn severity:

1. Tree mortality (%)–Mortality of all trees >10 cm DBH 1 year after a fire,
2. Soil heating–Average temperature in °C at 2 cm below the soil surface,
3. Fuel consumption–Total biomass of all fuels consumed during combustion (kg m^{-2}),
4. Fire intensity–Average fireline intensity for fire duration (kW m^{-1})

All variables in the statistical models utilizing simulated variables were also used in the construction of the integrated model.

We used multiple linear regression to model the relationships between CBI and the outputs from FIREHARM.

Table 2 Weather and fuel moisture values used as input to FIREHARM to predict fire severity (M = moisture of fuels and vegetation)

	Fire year	Max temp °C (°F)	Min temp °C (°F)	RelHum %	Wind speed km h^{-1} (m h^{-1})	Wind direction azimuth	Fuel moisture inputs								
							M 1 h %	M 10 h %	M 100 h %	M 1,000 h %	M foliar %	M litter %	M duff %	M herb %	M shrub %
Jocko Lakes	2007	22.1 (71.8)	11.9 (53.4)	35.8	11.1 (6.9)	260	11.8	10.4	6.9	11.0	100	11.8	58	30	69.1
MP boles Meadow	2003	33.1 (91.6)	8.9 (48.1)	22.9	7.9 (4.9)	225	14.6	13.0	8.4	15.2	100	14.6	56	51.1	79.4
Mineral Primm	2003	26.7 (80.1)	5.2 (41.4)	30.1	8.8 (5.4)	210	16.0	14.1	10.0	14.6	100	16.0	89	60.8	100.2
Cooney Ridge	2003	30.4 (86.8)	6.7 (44.0)	26.0	8.1 (5.0)	210	14.4	12.6	7.9	14.2	100	14.4	71	52.6	85.5
Kootenai Creek	2009	28.6 (83.5)	9.1 (48.4)	30.7	10.8 (6.7)	135	14.3	12.9	8.3	12.1	100	14.3	92	52.9	101.6
Gash Creek	2006	17.3 (63.2)	6.6 (43.9)	44.7	6.5 (4.0)	135	15.6	13.8	10.4	11.9	100	15.6	161	52.3	112.3
TarkioI90	2005	31.4 (88.5)	9.4 (48.8)	22.6	9.5 (5.9)	225	12.2	12.4	11.0	15.2	100	12.2	33	44.9	70.5
Gird End	2009	15.7 (60.2)	3.2 (37.8)	43.6	5.8 (3.6)	210	16.0	15.3	12.6	16.6	100	16.0	150	30.5	91.1
Bielenburg	2009	25.5 (77.9)	6.3 (43.4)	34.2	11.0 (6.8)	30	16.0	14.0	8.6	12.9	100	16.0	139	90.4	114.8
Lily Lake	2009	22.3 (72.1)	7.3 (45.1)	26.9	11.8 (7.3)	180	11.4	10.3	7.9	13.4	100	11.4	87	30.4	79.7
Flick Creek	2006	28.9 (84.0)	12.2 (53.9)	31.1	7.4 (4.6)	155	13.0	11.3	6.7	10.3	100	13.0	31	41.0	73.6
Tripod	2006	22.9 (73.3)	9.8 (49.7)	29.2	5.1 (3.2)	200	10.0	8.7	5.5	10.4	100	10.0	34	32.9	68.2
Tripod Spur	2006	23.8 (74.9)	10.4 (50.8)	29.0	5.0 (3.1)	200	9.9	8.8	5.2	9.5	100	9.9	43	39.9	71.5
Camel Humps	2008	29.1 (84.3)	13.3 (56.0)	29.3	8.0 (5.0)	155	11.9	11.0	11.6	22.2	100	11.9	24	37.3	64.3
Cold Springs	2008	29.0 (84.3)	8.6 (47.5)	22.5	9.2 (5.7)	315	12.6	10.6	7.6	12.7	100	12.6	28	85.7	85.9

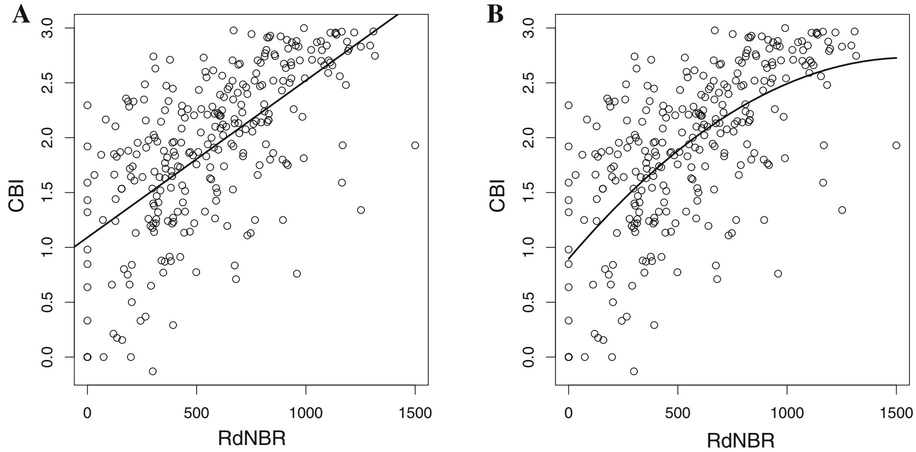

Fig. 3 Linear (**a**) and Nonlinear (**b**) relationship between CBI and RdNBR

Table 3 Evaluation statistics for RdNBR-based, Simulation-based, and Integrated models

Model	Estimate	Std. error	*t*-value	Pr(>|t|)	R^2	AIC	MSE
Simple Linear model (CBI ~ RdNBR)					0.417	477	0.306
Intercept	1.132	0.0639	17.470	<0.001			
RdNBR	0.0014	0.0001	14.210	<0.001			
Nonlinear model (CBI = a*RdNBR^2 + b*RdNBR + c)					0.424	476	0.302
a	−4.60E-07	2.34E-07	−1.961	0.05			
b	0.0019	0.0003	6.567	<0.001			
c	1.0001	0.0825	12.127	<0.001			
CBI ~ FIREHARM output variables only-full set of predictors					0.072	616	0.487
Intercept	1.8020	0.3622	4.974	<0.001			
Tree mortality	0.0047	0.0014	3.323	<0.01			
Soil heating	−0.0001	0.0022	−0.142	0.89			
Fuel consumption	−0.0033	0.0050	−0.647	0.52			
Intensity	0.0001	0.0001	1.194	0.23			
CBI ~ FIREHARM output variables only-Selected set of predictors					0.066	612	0.490
Intercept	1.5722	0.0870	18.080	<0.001			
Tree Mortality	0.0055	0.0012	4.457	<0.001			
CBI ~ FIREHARM output variables plus RdNBR-full set of predictors					0.479	453	0.273
Intercept	0.3745	0.2885	1.298	0.20			
Tree mortality	0.0042	0.0011	3.940	<0.01			
Soil heating	0.0020	0.0011	1.254	0.21			
Fuel consumption	0.0062	0.0016	1.611	0.10			
Intensity	0.0001	0.0001	1.057	0.29			
RdNBR	0.0014	0.0001	14.773	<0.001			
CBI ~ FIREHARM output variables plus RdNBR-Selected Set of Predictors					0.471	452	0.278
Intercept	0.8321	0.0827	10.066	<0.001			
Tree mortality	0.0050	0.0009	5.389	<0.001			
‘RdNBR	0.0014	0.0001	14.700	<0.001			

We present a model that includes all possible predictor variables, along with a model that includes only those predictors with statistical significance at $p < 0.05$, as determined through a stepwise multiple linear regression approach. Assessment of model residuals indicated that residuals were normally distributed for both simulated variables models (full model and selected variables model.)

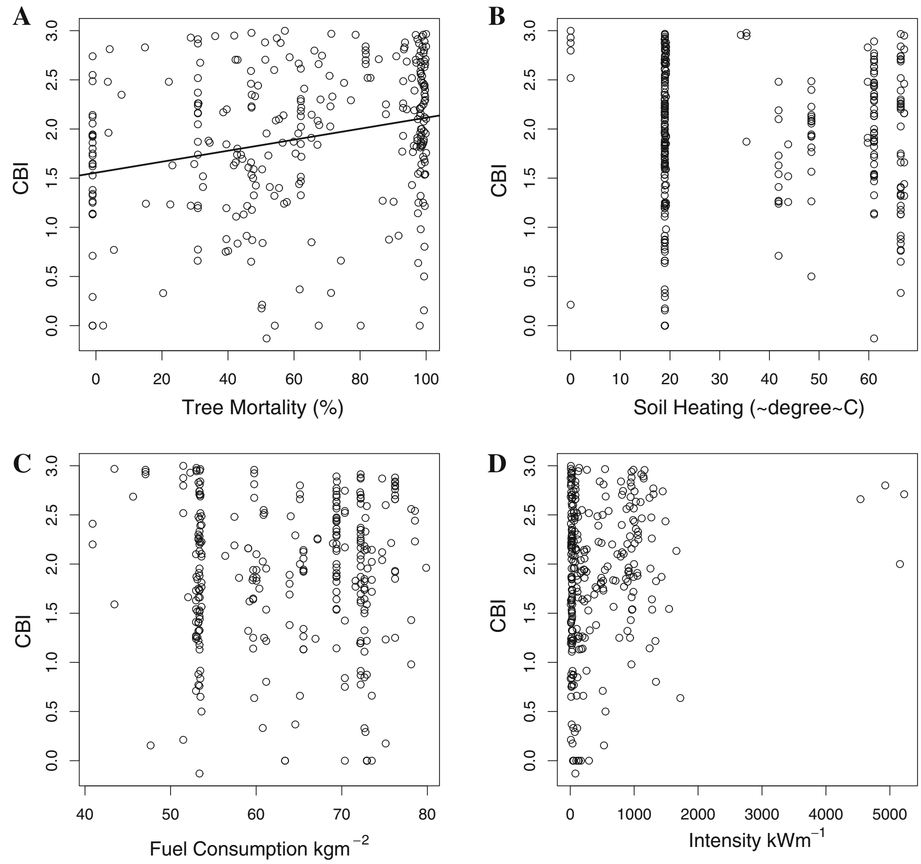

Fig. 4 Linear relationships between CBI and FIREHARM-simulated output variables: CBI and Tree Mortality (**a**), CBI and Soil Heating (**b**), CBI and Fuel Consumption (**c**), and CBI and Intensity (**d**)

Integrated Models

We also modeled the relationship between CBI, RdNBR, and the outputs from FIREHARM using multiple linear regression. For the integrated modeling process, RdNBR was forced into each tested model to ensure that the remote sensing element was part of the model equation. As in the simulation modeling approach, we present a full model, and one that uses a selected set of variables based on stepwise removal of nonsignificant predictors. Assessment of model residuals indicated that residuals were normally distributed for both integrated variables models (full model and selected variables model.)

Mapping

We generated digital maps of predicted CBI using the modeled relationships between CBI and RdNBR, CBI and FIREHARM-simulated variables, and the CBI and the Integrated Model. We classified field reference CBI and CBI as predicted by the three models, into severity categories corresponding to ranges in CBI values as outlined in Miller and Thode (2007),: "Unchanged" = 0 to 0.1, "Low" = 0.1–1.24,"Moderate" = 1.25–2.24, and "High" = 2.25–3.0. Using 10-fold cross-validation and classification error matrices, we quantified user's accuracy, producer's accuracy, overall map classification accuracy, and Kappa ($\hat{k}$) (Congalton and Green 1999) by comparing CBI as predicted by RdNBR, simulation, and integrated methods to field-measured CBI.

Results

RdNBR Linear and Nonlinear Statistical Models

For our data, CBI clearly increases with increasing values of RdNBR, and a nonlinear model appears to describe the relationship between CBI and RdNBR better than the linear model (Fig. 3). Furthermore, the nonlinear model had a slightly higher coefficient of determination than the linear model ($R^2 = 0.424$ versus $R^2 = 0.417$), and lower Akaike Information Criterion (AIC = 476 versus AIC = 477), but Mean Square Error was essentially the same (MSE = 0.302 versus MSE = 0.306) (Table 3).

Simulated Variables Statistical Models

Exploring the relationship between FIREHARM output variables and CBI, we found that simulated tree mortality generally increased with increasing CBI values, with a cluster of plots showing high CBI values corresponding

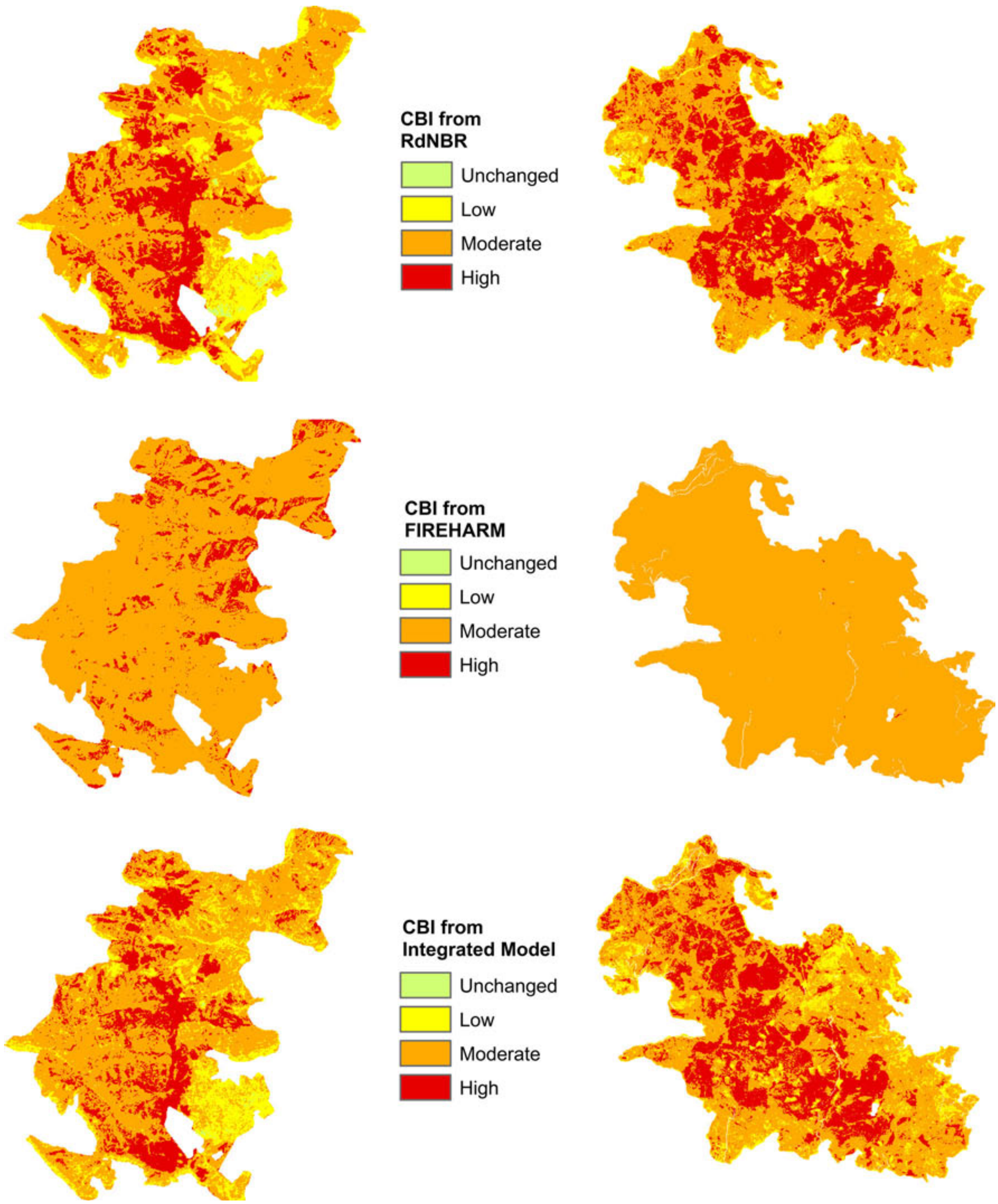

Fig. 5 Maps of predicted CBI for two example fires. *Left column*: Montana (Bielenburg), *Right column*: Washington (Tripod Complex). *Top Row*: CBI predicted from RdNBR simple linear model, *Middle row*: CBI predicted from FIREHARM-simulated model, *Bottom row*: CBI predicted from Integrated model

with maximum tree mortality (100 %) (Fig. 4). Correlation between CBI and simulated tree mortality was weak and positive ($r = 0.26$).There was not a clear relationship between CBI and any of the other FIREHARM-simulated output variables.

Models created with simulation output variables did not produce strong predictive relationships (Table 3). When all possible predictors were included in the model, only tree mortality was significant at $p < 0.05$, and it was the only variable included in the model determined by the stepwise multiple regression procedure. Coefficients of determination for the simulated variables models were low ($R^2 < 0.1$), and AIC and MSE values were high (AIC > 616 and MSE > 0.48.)

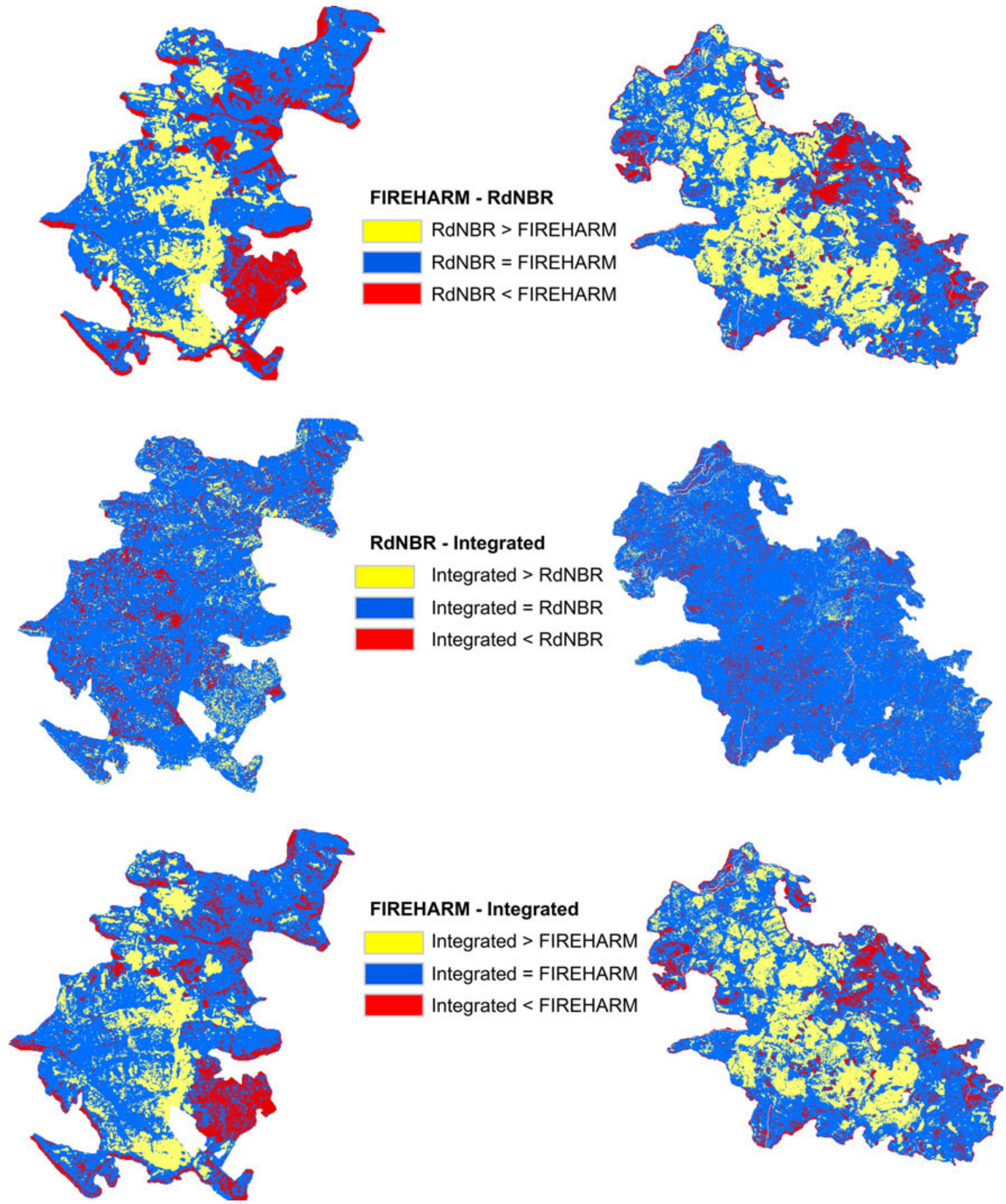

Fig. 6 Difference maps showing agreement and discrepancy between the three maps of predicted CBI for two example fires. *Left column*: Montana (Bielenburg), *Right column*: Washington (Tripod Complex). *Top row*: Difference between CBI predicted using FIREHARM-simulated variables and CBI predicted using RdNBR. *Middle Row*: Difference between CBI predicted from RdNBR and CBI predicted from the Integrated Model. *Bottom Row*: Difference between CBI predicted from RdNBR and CBI predicted from the Integrated Model

Integrated Statistical Models

Models that include both FIREHARM output variables along with RdNBR (Integrated Models), had the highest coefficients of determination and lowest AICs and MSEs of all models in the study ($R^2 > 0.47$) (Table 3).The Integrated Model with the full set of predictors that included all of the Simulated Model output variables plus RdNBR performed marginally better than the RdNBR model only. Similar to the Simulated Model situation, only tree mortality was significant at $p < 0.05$ in the Integrated Model that includes the full set of FIREHARM output

Table 4 Cross-tabulation of field-measured CBI (columns) and CBI as predicted by each of the three models in a 10-fold cross-validation (rows; RdNBR, FIREHARM Simulation, and Integrated Model)

	Unchanged	Low	Moderate	High	Row total	User's accuracy
RdNBR						
Overall Accuracy = 58.9 %, kappa = 0.30						
Unchanged	0	0	0	0	0	0 %
Low	6	6	9	1	22	27 %
Moderate	1	36	104	43	184	57 %
High	0	1	20	58	79	73 %
Column total	7	43	133	102	.	.
Producer's accuracy	0 %	14 %	78 %	57 %	.	.
Simulated Model						
Overall accuracy = 46.7 %, kappa = 0.00						
Unchanged	0	0	0	0	0	0 %
Low	0	0	0	0	0	0 %
Moderate	7	43	133	102	285	47 %
High	0	0	0	0	0	0 %
Column total	7	43	133	102	.	.
Producer's accuracy	0 %	0 %	100 %	0 %	.	.
Integrated Model						
Overall accuracy = 62.5 %, kappa = 0.36						
Unchanged	0	0	0	0	0	0 %
Low	4	8	7	4	23	35 %
Moderate	3	34	113	41	191	60 %
High	0	1	13	57	71	80 %
Column total	7	43	133	102	.	.
Producer's accuracy	0 %	19 %	85 %	56 %	.	.

variables. The integrated model as selected from the stepwise multiple regression procedure includes tree mortality as modeled from FIREHARM and RdNBR. Both the Integrated Model using the full set of FIREHARM output and the model using the selected predictors have similar coefficients of determination, AIC, and MSE (Table 3).

Map Comparison

Maps were created using 1) the nonlinear CBI-RdNBR model, 2) the Simulated Model that includes the selected set of predictors, and 3) the Integrated Model with the selected set of predictors (Figs. 5, 6). Visual comparison of the three fire severity maps showed that each method produced different patterns of predicted CBI across the landscape (See Fig. 5, for examples of predicted CBI maps for two fires, one in Montana and one in Washington). The moderate burn severity category dominates maps of CBI as predicted by FIREHARM outputs. Difference maps further substantiate discrepancies in spatial patterns of CBI as predicted from the three models, however; maps created by RdNBR, and the Integrated Model are quite similar (Fig. 6).

Error matrices show that the Integrated model had the strongest overall map accuracy with CBI field-measured plots (62.5 %) and the strongest kappa (0.36), followed by the RdNBR model (accuracy = 58.9 %, kappa = 0.30). The map created with the Simulated Model had the weakest overall accuracy (46.7 %) and kappa (0.00) (Table 4). The Simulated Model had a very high producer's accuracy for the moderate burn severity class (100 %); however, the user's accuracy was only 47 % for this class. The Integrated Model showed a similar pattern, with a high producer's accuracy for the moderate category (85 %), and a moderate user's accuracy for that category (60 %). For the high severity class, among all predictive models in the study, the Integrated Model had the highest user's accuracy (80 %), while the RdNBR Model had the highest producer's accuracy (57 %) for that category.

Discussion

In this study, we explored the capability of a fire effects simulation model to add value to spatial burn severity assessments across forested landscapes; a process traditionally conducted using satellite imagery alone. While we found the addition of simulated variables improves severity mapping, we also found that the strengths and weaknesses in both RdNBR and simulation approaches also exist for the integrated approach.

We chose RdNBR as our image-based burn severity mapping method, because it is a measure of change that is relative to pre-fire conditions, and thereby ostensibly affords consistency across regions (Miller and Thode 2007). However, the coefficients of determination that we found for the relationship between RdNBR and CBI were lower than those reported in other RdNBR studies throughout a variety of ecosystem types (Miller et al. 2009a, b; Miller and Thode 2007; Dillon et al. 2011a; Zhu et al. 2006; Cansler and McKenzie 2012; Soverel et al. 2010). Regardless, RdNBR was more successful at predicting burn severity than the simulated variables were used in this study.

There are likely several reasons why the regression relationships between CBI and the FIREHARM-simulated variables were weak. FIREHARM uses the latest fire behavior and effects modeling technology in an integrated platform. The algorithms at the core of the model are based upon empirical studies or physical processes, and the FOFEM model is well vetted and has been used extensively in fire effects research and management. However, FIREHARM is a research tool currently under assessment for management applicability, and it does have some limitations: (1) FIREHARM always simulates a "head" fire (a fire that spreads with the wind) which may lead to overestimation of fire intensity in situations where flanking or backing fires are more likely, (2) it does not address spatial relations (what happens in one pixel is independent of what happened in surrounding pixels), (3) input parameters may not match the scale of analysis (e.g., fuel moisture content is specified for broad areas, but moistures are highly variable locally). Lastly, and perhaps most importantly, FIREHARM performance ultimately depends on accurate spatial inputs, and it appears LANDFIRE mapping products likely contain a high level of uncertainty (Keane et al. 2013, 2006; Krasnow et al. 2009; Reeves et al. 2009); fuel loadings from the LANDFIRE FLM map are inaccurate because (1) surface fuel characteristics vary at finer scales than the FLM map (Keane et al. 2012) (2) FLMs were created from a limited dataset (Lutes et al. 2009), (3) FLM mapping involved assigning an FLM to a vegetation type, but fuels are rarely correlated to vegetation conditions (Keane et al. 2013), and the vegetation type categories were too broad for consistent and accurate FLM assignment (Keane et al. 2006). The accuracy of the LANDFIRE Tree List product is questionable for similar reasons: (1) scale of variation in Forest Inventory Analysis (FIA) tree data did not match the resolution of vegetation type categories and LANDFIRE maps, (2) assignment of FIA plots to vegetation types was incomplete, because there was not a tree list for every vegetation type category, and (3) the tree data was not rectified with the FLM fuels data (Drury and Herynk 2011). To adequately improve the LANDFIRE fuel model and tree list mapping products, the weaknesses, as described above, would need to be addressed. Perhaps if the scale discrepancies between the fuels and tree information and map resolution were reconciled, and if sufficient field reference data were available to adequately characterize these variables, the map product accuracy would increase, and FIREHARM simulation output would correspondingly improve.

Along with improved surface and canopy spatial information, finer scale weather inputs would likely increase simulation model performance. In this study, weather stations used to estimate fuel conditions were often distant from the fire (up to 96 km).

We also suspect that one of the primary reasons for the weak relationships between modeled variables and CBI is that the continuous simulated variables were used to compute a qualitative, categorical index that was then compared to CBI. FIREHARM predicts biophysically dimensioned, individual fire effects that are not intended as an integrated assessment of burn severity. Karau and Keane (2010) showed that FIREHARM successfully predicted surface fuel consumption spatially, but when model outputs are pooled in attempt to relate them to an integrative measure, such as CBI, the discrete information that the model provides about each specific effect is diluted. CBI tends to be tree-canopy centric, which is likely why tree mortality output from FIREHARM was the only significant predictor in the models that we tested.

It is not surprising that overall map agreement was greatest between maps created with RdNBR, and the Integrated Model as RdNBR is a major component of the Integrated Model. Map accuracy assessment results demonstrate the utility of an integrated burn severity mapping methodology. These results mimic regression model results in that the Integrated Model accuracies were strongest, RdNBR Model accuracies were intermediate, and Simulated Model accuracies were weakest; the Integrated Model is more successful at mapping burn severity than the other methods. The high user's accuracy for the high severity class in the Integrated model is noteworthy; this result indicates that this model could prove useful for managers wishing to identify critical areas threatened by post-fire damage (e.g., Burned Area Emergency Response teams).

A problem with the general concept of "burn severity" is that a researcher or manager might be interested in specific aspects of how a landscape is changed by fire; however, it is cumbersome to compare a specific fire effect to an index that integrates soil, substrates, herbs, shrubs, intermediate trees, and large trees (French et al. 2008; Morgan et al., in review). So, a proxy for burn severity, such as CBI or RdNBR, may be too broad to be useful for all situations. Managers may, in some situations, need to spend time and resources to complete field evaluations of specific fire effects like tree mortality, fuel consumption, and soil damage. However, a broad, integrative measure of burn severity is sometimes desirable, if only to generate a map that facilitates broad-scale rehabilitation prioritization. Our results show that a combination of satellite information and simulation modeling does a reasonable job of capturing CBI for these purposes.

Conclusion

The results of Karau and Keane (2010) and the present study demonstrate the potential utility of a fire effects simulation model to predict individual fire effects (e.g., fuel consumption) used in tandem with satellite imagery to predict an integrated measure of burn severity at forest landscape scales, though the system is still in research mode. FIREHARM can provide estimates of surface fire effects whereas imagery-based assessments are canopy centric. So, despite model limitations and data quality challenges, we feel that the extra effort required to implement FIREHARM is warranted when the user needs information about surface fire effects.

Although the relationships that we found between landscape-scale burn severity estimates (satellite-based, modeled, and integrated) were generally not very strong, we were encouraged to see any performance gains from the integrated model, given the poor accuracy of the FIREHARM input data. We suspect that with higher quality and more accurate spatial input data, the performance of the simulation model could greatly improve, as would the integrated burn severity product. In the present study, we wished to assess the potential of an integrated burn severity mapping process that uses spatial data that are readily available to land managers; however, we suggest that future model users scrutinize input data and familiarize themselves with data limitations.

Replicating this study on small landscapes with accurate, local level model input data and local weather would allow further investigation of how data challenges limit the integrated mapping approach. An added benefit of using more accurate model input data is that FIREHARM could be used prior to a fire event to estimate potential fire effects, enabling strategic resource allocation to areas with high potential for damage. With highly accurate input data, we believe that integrating image-based and simulation-based models for mapping burn severity, as well as using simulation to provide maps of individual fire effects, could provide fire managers with an innovative suite of tools to assess the effects of fire on their landscapes, understand the processes behind fire severity, and interpret severity maps in an appropriate context.

Acknowledgments This research was supported in part by the Joint Fire Sciences Program (Project 09-1-07-4), and by the Rocky Mountain Research Station Fire Modeling Institute. We would like to thank the following people: Jason Herynk, Signe Leirfallom, Aaron Sparks, Brian Izbicki, Christy Lowney, Amy Olson, Stacy Drury, Susan Prichard, Alina Cansler, Karen Kopper, Tony Guay, Faith Ann Heinsch and L. Scott Baggett. We also thank the editors and three anonymous reviewers whose comments greatly improved the manuscript.

References

Anderson HE (1982) Aids to determining fuel models for estimating fire behavior. General Technical Report INT-122. U.S. Department of Agriculture, Intermountain Forest and Range Experimental Station, Ogden, UT

Bradshaw LS, Tirmenstein D (2010) FireFamilyPlus users guide, version 4.1 (Draft). In: U.S. Department of Agriculture Forest Service, Fire Sciences Laboratory, Missoula

Cansler CA (2011) Drivers of burn severity in the northern Cascade Range, Washington. Master of Science, University of Washington, Washington

Cansler CA, McKenzie D (2012) How robust are burn severity indices when applied in a new region? Evaluation of alternate field-based and remote-sensing methods. Remote Sens 4:456–483

Carlson JD, Bradshaw LS, Nelson RM, Bensch RR, Jabrzemski R (2007) Application of the Nelson model to four timelag fuel classes using Oklahoma field observations: model evaluation and comparison with National Fire Danger Rating System algorithms. Int J Wildland Fire 16:204–216

Chuvieco E, Riano D, Danson FM, Martin P (2006) Use of a radiative transfer model to simulate the postfire spectral response to burn severity. J Geophys Res 111:G04S09

Cocke AE, Fule PZ, Crouse JE (2005) Comparison of burn severity assessments using Differenced Normalized Burn Ratio and ground data. Int J Wildland Fire 14:189–198

Collins BM, Kelly M, van Wagtendonk JW, Stephens SL (2007) Spatial patterns of large natural fires in Sierra Nevada wilderness areas. Landsc Ecol 22:545–557

Congalton RG, Green K (1999) Assessing the accuracy of remotely sensed data: principles and practices. CRC/Lewis Press, New York

De Santis A, Chuvieco E, Vaughan PJ (2009) Short-term assessment of burn severity using the inversion of PROSPECT and GeoSail models. Remote Sens Environ 113:126–136

De Santis A, Asner GP, Vaughan PJ, Knapp DE (2010) Mapping burn severity and burning efficiency in California using simulation models and Landsat imagery. Remote Sens Environ 114: 1535–1545

Dillon GK, Holden ZA, Morgan P, Crimmins MA, Heyerdahl EK, and Luce CH, (2011a) Both topography and climate affected forest and woodland burn severity in two regions of the western US, 1984 to 2006. Ecosphere 212: article 130

Dillon G, Morgan P, Holden Z (2011b) Mapping the potential for high severity wildfire in the western United States. Fire Manag Today 71:25–28

Drury SA, JM Herynk (2011) The national tree-list layer. General Technical Report RMRS-GTR 254. U.S. Department of Agriculture Forest Service, Rocky Mountain Research Station, Fort Collins, CO

Eidenshink J, Schwind B, Brewer K, Zhu Z, Quayle B, Howard S (2007) A project for monitoring trends in burn severity. Fire Ecol 3:3–21

Epting J, Verbyla D (2004) Landscape-level interactions of prefire vegetation, burn severity, and postfire vegetation over a 16-year period in interior Alaska. Can J For Res 35:1367–1377

French NH, Kasischke ES, Hall RJ, Murphy KA, Verbyla DL, Hoy EE, Allen JL (2008) Using Landsat data to assess fire and burn severity in the North American Boreal forest region: and overview and summary of results. Int J Wildland Fire 17:443–462

Haire SL, McGarigal K (2009) Changes in fire severity across gradients of climate, fire size, and topography: a landscape ecological perspective. Fire Ecol 5:86–103

Holden ZA, Morgan PA, Evans JS (2009) A predictive model of burn severity based on 20-years of burn severity data in a large Southwestern US wilderness area. For Ecol Manag 258:2399–2406

Hudak AT, Morgan PA, Bobbit MJ, Smith AMS, Lewis SA, Lentile LB, Robichaud PR, Clark JT, McKinley RA (2007) The relationship of multispectral satellite imagery to immediate fire effects. Fire Ecol 3:64–90

Jensen JR (1983) Biophysical remote sensing. Ann Assoc Am Geogr 73:111–132

Karau EC, Keane RE (2010) Burn severity mapping using simulation modeling and satellite imagery. Int J Wildland Fire 19:710–724

Keane RE, Frescino TL, Reeves MC and Long J (2006) Mapping wildland fuels across large regions for the LANDFIRE prototype project. In: Rollins MG, Frame C (eds) The LANDFIRE prototype project: nationally consistent and locally relevant geospatial data for wildland fire management. General Technical Report RMRS-GTR-175. US Department of Agriculture, Forest Service, Rocky Mountain Research Station, Fort Collins, CO

Keane RE, Drury SA, Karau EC, Hessburg PF, Reynolds KM (2010) A method for mapping fire hazard and risk across multiple scales and its application in fire management. Ecol Model 221:2–18

Keane R, Gray K, Bacciu V, Leirfallom S (2012) Spatial scaling of wildland fuels for six forest and rangeland ecosystems of the northern Rocky Mountains, USA. Landsc Ecol 27:1213–1234

Keane RE, Herynk JM, Toney C, Urbanski SP, Lutes DC, Ottmar RD (2013) Evaluating the performance and mapping of three fuel classification systems using Forest Inventory Analysis surface fuel measurements. For Ecol Manag 305:248–263

Keeley JE, Brennan T, Pfaff AH (2008) Fire severity and ecosystem responses following crown fires in California shrublands. Ecol Appl 18:1530–1546

Key CH, Benson NC (2006a) Landscape assessment: remote sensing of severity, the Composite Burn Index. In: Lutes DC, Keane RE, Caratti JF, Key CH, Benson NC Ganji LJ (eds) 'FIREMON': Fire effects monitoring and inventory system. General Technical Report RMRS-GTR-164. Department of Agriculture, Forest Service, Rocky Mountain Research Station, Ogden, UT

Key CH, Benson NC (2006b) Landscape assessment: remote sensing of severity, the Normalized Burn Ratio. In: Lutes DC, Keane RE, Caratti JF, Key CH, Benson NC Ganji LJ (eds) 'FIREMON': Fire effects monitoring and inventory system. General Technical Report RMRS-GTR-164. Department of Agriculture, Forest Service, Rocky Mountain Research Station, Ogden, UT

Kopper K (2012) Frequency and severity of a mixed-severity fire regime: the Douglas fir/Ponderosa pine forests of Stehekin, Washington, USA. Dissertation, University of Washington

Krasnow K, Schoennagel T, Veblen TT (2009) Forest fuel mapping and evaluation of the LANDFIRE fuel maps of Boulder County, Colorado, USA. For Ecol Manag 257:1603–1612

Lutes DC, Keane RE, Caratti JF (2009) A surface fuels classification for estimating fire effects. Int J Wildland Fire 18:802–814

McNab WH, Avers PE (1994). Ecological subregions of the United States: section descriptions. Administrative Publication WO-WSA-5, USDA Forest Service, Washington, DC

Miller JD, Thode AE (2007) Quantifying burn severity in a heterogeneous landscape with a relative version of the delta Normalized Burn Ratio (dNBR). Remote Sens Environ 109:66–80

Miller JD, Knapp EE, Key CH, Skinner CN, Isbell CJ, Creasy RM, Sherlock JW (2009a) Calibration and validation of the relative differenced Normalized Burn Ratio (RdNBR) to three measures of fire severity in the Sierra Nevada and Klamath Mountains, California, USA. Remote Sens Environ 113:645–656

Miller JD, Safford HD, Crimmins M, Thode AE (2009b) Quantitative evidence for increasing forest fire severity in the Sierra Nevada and Southern Cascade mountains, California and Nevada, USA. Ecosystems 12:16–32

Morgan PA, Keane RE, Dillon GK, Karau EC, Sikkink P, Silverstein R. The problem with fire severity and its application in fire management. Int J Wildland Fire (in review)

Nelson RM (2000) Prediction of diurnal change in 10-h fuel stick moisture content. Can J For Res 30:1071–1087

Prichard S, Peterson DL, Jacobson K (2010) Fuel treatments reduce the severity of wildfire effects in dry mixed conifer forests, Washington, USA. Can J For Res 40:1615–1626

Reeves MC, Kost JR, Ryan KC (2006) Fuels products of the LANDFIRE project. In: Andrews PL, Butler BW (eds) Fuels management–how to measure success. Proceedings RMRS-P-41. US Department of Agriculture, Forest Service, Rocky Mountain Research Station, Fort Collins, CO

Reeves MC, Ryan KC, Rollins MC, Thompson TG (2009) Spatial fuel data products of the LANDFIRE project. Int J Wildland Fire 18:250–267

Reinhardt E, Keane RE, Brown JK (1997) First Order Fire Effects Model: FOFEM 4.0 User's Guide. General Technical Report INT-GTR-344. US Department of Agriculture, Forest Service, Intermountain Research Station, Ogden, UT

Rollins MG (2009) LANDFIRE: a nationally consistent vegetation, wildland fire, and fuel assessment. Int J Wildland Fire 18:235–249

Sikkink P, Keane RE, Lutes DC (2009). Field guide for identifying fuel loading models. General Technical Report RMRS-GTR-225. US Department of Agriculture, Forest Service, Rocky Mountain Research Station, Fort Collins, CO

Soverel NO, Perrakis DDB, Coops NC (2010) Estimating burn severity from Landsat dNBR and RdNBR indices across western Canada. Remote Sens Environ 114:1896–1909

R Development Core Team (2010) R: A language and environment for statistical computing; R foundation for statistical computing: Vienna, Austria. http://www.R-project.org/. Accessed Feb 2014

Van Wagner CE, Pickett TL (1985) Equations and FORTRAN program for the Canadian Forest Fire Weather Index System. Forestry Technical Report 33. Canadian Forestry Service, Ottawa, Ontario

Van Wagtendonk JW, Root RR, Key CH (2004) Comparison of AVIRIS and Landsat ETM+ detection capabilities for burn severity. Remote Sens Environ 92:397–408

Western Regional Climate Center (2012) RAWS USA Climate Archive. Desert Research Institute, Reno, NV. http://www.raws.dri.edu/index.html. Accessed Feb 2014

Zhu Z, Key C, Ohlen D, Benson N (2006) Evaluate sensitivities of burn-severity mapping algorithms for different ecosystems and fire histories in the United States. Final Report JFSP 01-1-4-12. Joint Fire Sciences Program